ACS Catalysis

Research Article

pubs.acs.org/acscatalysis

Improved Postsynthesis Strategy to Sn-Beta Zeolites as Lewis Acid Catalysts for the Ring-Opening Hydration of Epoxides

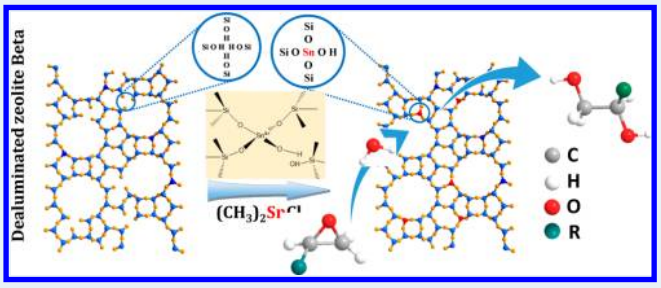
Bo Tang,[†] Weili Dai,[†] Guangjun Wu,[†] Naijia Guan,[†] Landong Li,*[,†] and Michael Hunger[‡]

[†]Key Laboratory of Advanced Energy Materials Chemistry (Ministry of Education), College of Chemistry, Nankai University, No. 94 Weijin Road, Tianjin 300071, People's Republic China

[‡]Institute of Chemical Technology, University of Stuttgart, Pfaffenwaldring 55, 70550 Stuttgart, Germany

Supporting Information

ABSTRACT: Nanocrystalline Sn-Beta zeolites have been successfully prepared via an improved two-step postsynthesis strategy, which consists of creating vacant T sites with associated silanol groups by dealumination of parent H-Beta and subsequent dry impregnation of the resulting Si-Beta with organometallic dimethyltin dichloride. Characterization results from UV−vis, XPS, Raman, and ^{119}Sn solid-state MAS NMR reveal that most Sn species have been successfully incorporated into the framework of Beta zeolite through the postsynthesis process and exist as isolated tetrahedral Sn(IV) in open arrangement. The creation of strong Lewis acid sites upon Sn incorporation is confirmed by FTIR spectroscopy with pyridine adsorption. The Sn-Beta Lewis acid catalysts are applied in the ring-opening hydration of epoxides to the corresponding 1,2-diols under near ambient and solvent-free conditions, and remarkable activity can be obtained. The impacts of Lewis acidity, preparation parameters, and reaction conditions on the catalytic performance of Sn-Beta zeolites are discussed in detail.



KEYWORDS: *Sn-Beta, postsynthesis, organometallic, epoxide, ring-opening hydration*

1. INTRODUCTION

Epoxides are important and well-known carbon electrophiles that can be industrially produced from the corresponding olefin precursors.[1] As a result of the three-membered heterocyclic ring strain of the epoxides, nucleophiles can attack the electrophilic carbon atom of the C−O bond and break the bond, thereby resulting in its ring-opening. Generally, it is susceptible to attacks by a range of nucleophiles, including nitrogen (e.g., ammonia, amines, and azides), oxygen (e.g., water, alcohols, phenols, and acids) and sulfur-containing compounds, producing bifunctional molecules for great chemical industry.[2,3] Especially, 1,2-diols, produced from the direct ring-opening hydration of epoxides as the most straightforward approach, are widely used as intermediates for the manufacture of polyester resins, antifreezes, cosmetics, medicines, and other products.[4] The hydration of epoxides is generally carried out with a large excess of water (H_2O/epoxide = 20−25) at elevated temperature (>413 K) and/or in the presence of solvents to obtain high substrate conversion as well as desired product selectivity. Specially, the concentration of the product in the final aqueous solution is only 10 wt %, and huge energy is consumed for the distillation of the product from the aqueous solution, making the epoxide hydration one of the most cost- and energy-intensive processes in the chemical industry. Various acids and bases (e.g., cation- and anion-exchange resins,[5−8] quaternary phosphonium halides,[9] polymeric organosilane ammonium salts,[10] macrocyclic chelating compounds,[11] cyclic amine,[12] supported metal oxides,[13,14] and silica-based nanoreactors)[15] have been developed to catalyze the ring-opening hydration of epoxides. Despite current achievements, efficient and recyclable catalytic systems that can work under mild reaction conditions are yet to be explored.

Lewis acids represent a versatile class of catalysts that exhibit remarkable activity in a number of important chemical transformations.[16,17] Compared with homogeneous analogues, heterogeneous Lewis acid catalysts offer several advantages for the development of more sustainable technology in terms of facile downstream processing and process intensification and, therefore, attract extensive attention. The exploitation of Sn-Beta zeolites, Sn(IV) incorporation into the BEA framework structure, can be viewed as a key breakthrough in the search of environmental-friendly solid Lewis acid catalysts for sustainable chemistry. Sn-Beta zeolites have been successfully applied in several very important reactions (e.g., Baeyer−Villiger oxidations[18] and Meerwein−Ponndor−Verley reductions).[19] A most interesting feature of Sn-Beta zeolites is that the Lewis acid sites processed are tolerant to polar and protic solvents (e.g., water and alcohols) being essentially different from most conventional solid Lewis acid catalysts.[17] Accordingly, remarkable catalytic performance of Sn-Beta zeolite in carbohydrate-related reactions in aqueous media (e.g., sugar isomer-

Received: April 28, 2014
Revised: July 15, 2014
Published: July 23, 2014

 © 2014 American Chemical Society dx.doi.org/10.1021/cs500891s | ACS Catal. 2014, 4, 2801−2810

ization,[20−22] epimerization,[23] and Cannizzaro-type reactions)[24,25] has been recently reported.

Generally, Sn-Beta zeolites can be prepared by the direct incorporation of Sn species into a BEA framework during hydrothermal synthesis.[26] Considerable long time scale of up to 40 days is required to realize a full crystallization to overcome the negative effect from the existence of Sn(IV), and additive fluoride is commonly employed to facilitate the crystallization process,[23,27] resulting in both a lack of reproducibility and feasibility for large-scale synthesis. Accordingly, a much more rapid hydrothermal strategy has been reported to synthesize Sn-Beta material in 2 days using a modified seeding method, but it still involves the environmentally unfriendly HF media and results in the formation of large crystallites.[28] In this context, alternative postsynthesis strategies have been proposed for the preparation of Sn-Beta zeolites,[29−32] in which a commercial Beta zeolite is dealuminated to generate silanols prior to grafting Sn species. Wu et al. conducted the incorporation of Sn ions into the vacant tetrahedral sites of Beta by the so-called "atom-planting method" using $SnCl_4$ vapor;[29] however, formation of large quantities of inactive bulk SnO_2 could not be avoided. Alternatively, a simple grafting procedure in isopropanol at elevated temperature was reported by Sels et al. for preparing a highly active Sn-Beta zeolite,[30] in which the incorporation of a significant amount of Lewis acid is still challenging. More recently, the exploration of solid-state ion exchange route involving dealuminated Beta and tin(II)-acetate by the Hermans group provides a potential strategy to prepare Sn-Beta with high Sn loading up to 10 wt % without the formation of bulk SnO_2,[31] which could be further extended to the preparation of Ti-Beta and Zr-Beta.[32]

Inspired by the above-mentioned approaches, we, herein, will report an improved two-step postsynthesis procedure for the preparation of Sn-beta zeolites based on the dry impregnation of dealuminated zeolite Beta with organometallic precursor dimethyltin dichloride. The formation of isolated Sn(IV) Lewis acid sites in nanocrystalline Sn-Beta zeolites is guaranteed, and the obtained Sn-Beta zeolites are, for the first time, applied in the ring-opening hydration of epoxides to the corresponding 1,2-diols. The excellent catalytic performance obtained demonstrates the great potential of heterogeneous Lewis acid (e.g., Sn-Beta) in the ring-opening addition of epoxides.

2. EXPERIMENTAL SECTION

2.1. Sample Preparation. Epichlorohydrin (99%), styrene oxide (>98%), cyclohexene oxide (>98%), ethylene oxide (99%), propylene oxide (>99%), epoxybutane (>98%), dimethyltin dichloride (98%), titanocene dichloride (>99%), and zirconocene dichloride (>99%) were purchased from Alfa Aesar and used as received without further purification.

Sn-Beta zeolites were prepared through a two-step postsynthesis procedure, which consisted of the dealumination of parent H-Beta and then incorporation of Sn species into the framework of dealuminated Si-Beta via dry impregnation and calcination. Briefly, commercial Beta zeolite with nominal n_{Si}/n_{Al} ratio of 13.5 (Sinopec Co.) was stirred in a 13 mol L^{-1} nitric acid aqueous solution (20 mL $g_{zeolite}^{-1}$) at 373 K overnight to obtain a dealuminated Beta (Si-Beta). The powder was filtered, washed thoroughly with deionized water, and dried at 353 K overnight. Before the incorporation of Sn, the sample was pretreated at 473 K overnight under vacuum to remove physisorbed water. Afterward, 1.0 g of the solid powder was finely ground with appropriate amount of $(CH_3)_2SnCl_2$ in the glovebox to achieve an intimate mixture with the n_{Si}/n_{Sn} ratio of 40, 50, and 100, respectively. The solid mixture was put into a tubular reactor, then sealed and heated to 823 K for 6 h (heating rate at 5 K/min) under vacuum. After that, it was calcined under flowing air at 823 K for 6 h to derive the final product, denoted as Sn-Beta-*X* where *X* indicates the n_{Si}/n_{Sn} ratio.

Zr-Beta and Ti-Beta were prepared via procedures similar to that for Sn-Beta except that the organometallic precursor $(CH_3)_2SnCl_2$ was replaced by Cp_2ZrCl_2 and Cp_2TiCl_2, respectively. In addition, the Si-Beta supported oxides (i.e., SnO_2/Si-Beta, ZrO_2/Si-Beta, and TiO_2/Si-Beta) were prepared via mechanical mixing of Si-Beta with corresponding metal oxides, followed by calcination at 823 K for 12 h to derive the corresponding products.

2.2. Characterization Techniques. X-ray diffraction (XRD) patterns of samples were recorded on a Bruker D8 diffractometer with Cu Kα radiation (λ = 1.54184 Å) from 5° to 40° with a scan speed of 2θ = 6.0°/min.

Scanning electron microscopy (SEM) images of samples were obtained on a Hitachi S-4800 microscope.

The chemical compositions of samples were determined by inductively coupled plasma emission spectrometry (ICP-AES) on a Thermo IRIS Intrepid II XSP atomic emission spectrometer.

The surface areas and pore volumes of the calcined samples were measured by means of nitrogen adsorption at 77 K on a QuantachromeiQ-MP gas adsorption analyzer. Before the nitrogen adsorption, samples were dehydrated at 473 K for 6 h. The total surface area was calculated via the Brunauer−Emmett−Teller (BET) equation, and the microporous pore volume was determined using the *t*-plot method.

Diffuse reflectance ultraviolet−visible (UV−vis) spectra of dehydrated samples were recorded against $BaSO_4$ in the region of 200−700 nm on a Varian Cary 300 UV−vis spectrophotometer.

Raman spectra of dehydrated samples were recorded on a high-resolution, dispersive Raman spectrometer system (Horiba-JobinY-vonLabRam-IR) with the He−Cd laser (Kimmon Electric, model IK57511-G; 441.6 nm output power of 110 mW, sample power of 28 mW).

X-ray photoelectron spectra (XPS) of dehydrated samples were recorded on a Kratos Axis Ultra DLD spectrometer with a monochromated Al Kα X-ray source ($h\nu$ = 1486.6 eV), hybrid (magnetic/electrostatic) optics, and a multichannel plate and delay line detector (DLD). All spectra were recorded by using an aperture slot of 300 × 700 μm. Survey spectra were recorded with a pass energy of 160 eV and high-resolution spectra with a pass energy of 40 eV. Accurate binding energies (±0.1 eV) were determined with respect to the position of the adventitious C 1s peak at 284.8 eV.

Diffuse reflectance infrared Fourier transform (DRIFT) spectra of samples were measured on a Bruker Tensor 27 spectrometer with 128 scans at a resolution of 2 cm^{-1}. A self-supporting pellet made of sample material was placed in the reaction chamber and pretreated in flowing dry air at 673 K for 1 h. The spectra were recorded in dry air against KBr as background.

Fourier transform infrared (FTIR) spectra of pyridine adsorption were also collected on the Bruker Tensor 27 spectrometer. A self-supporting pellet made of the sample was placed in the flow cell and evacuated under reduced pressure at 693 K for 4 h. After cooling to room temperature, the samples were saturated with pyridine vapor and then evacuated at 473, 573, or 623 K for 30 min. Spectra were recorded at evacuation temperature in the 4000−650 cm^{-1} range by using coaddition of 32 scans. The amount of the Lewis acid sites in samples was determined from the integral intensity of characteristic band at ca. 1450 cm^{-1} using the molar extinction coefficients of Emeis.[33]

The ^{119}Sn solid-state magic angle spinning nuclear magnetic resonance (MAS NMR) experiments were performed on a Bruker Avance III spectrometer at resonance frequencies of 149.5 MHz and with a sample spinning rate of 8 kHz. ^{119}Sn MAS NMR spectra of Sn-Beta were recorded on dehydrated samples, which were obtained by heating the samples at 673 K at a pressure below 10^{-2} Pa for 6 h.

2.3. Catalytic Evaluation. The catalytic processes for epoxides hydration were performed in a 25 mL round-bottom glass flask with a cryogenic-liquid condenser under atmospheric pressure. The vessel was charged with the mixture of 10 mmol of epoxide, 20 mmol of H_2O, and 0.1 g of catalyst, and mixed vigorously by a magnetic stirrer.

dx.doi.org/10.1021/cs500891s | ACS Catal. 2014, 4, 2801−2810

After the reaction, samples of the reaction were qualitatively analyzed by Shimadzu 2010 GC (Agilent HP-5MS column, 30 m × 0.25 mm × 0.25 μm; FID detector) with octanol as the internal standard. GC peaks were identified by comparison with the retention time of known standard samples, and also by means of Shimadzu GC-MS QP2010 SE equipped with the Agilent HP-5MS column. Carbon balance of over 95% was obtained for all experiments.

A hot-filtration test was performed to confirm the heterogeneous nature of the catalyst under the identical conditions employed for the catalytic hydration reaction. The solid was removed from the reaction mixture after 1 h by centrifugation and subsequently filtered over a syringe filter. Then, the filtrate was allowed to react for another 5 h.

To verify the potential recyclability of Sn-Beta catalyst, recycling tests were performed. After reaction completion, the sample was centrifuged at 6000 rpm to deposit the solid catalyst. The solid catalyst was directly reused for next cycle. After the fourth cycle, the solid catalyst was washed with 5 mL of acetone for three times, dried at 393 K overnight, and subjected to calcination at 823 K for 6 h for reuse in the next cycle.

3. RESULTS AND DISCUSSION

3.1. Incorporation of Sn into Zeolite Framework. To verify the possible structure changes during the postsynthesis procedures, the XRD patterns of the parent H-Beta and post-treated samples are collected in Figure 1. All the samples show

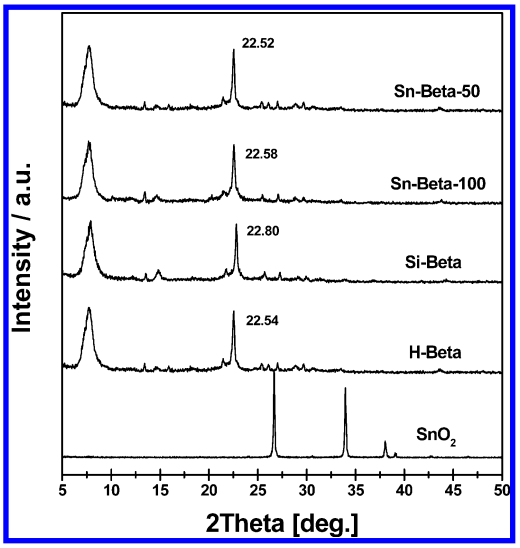


Figure 1. XRD patterns of H-Beta, Si-Beta, Sn-Beta, and SnO_2 samples.

similar diffractions peaks characteristic of typical BEA topology with the comparable intensity, ruling out the obvious collapse of zeolite framework during the dealumination and Sn incorporation, in line with earlier reports.[29−31] The dealumination and incorporation of Sn species into the zeolite framework of Beta should be accompanied by the contraction/expansion of the framework and therefore result in detectable changes in the position of the diffraction peak (302) at 2θ = 22.5°, as reported by Dzwigaj et al.,[34,35] considering the difficulty in determining the unit cell parameters in Beta zeolite due to the coexistence of several polytypes.[36] As shown in Figure 1, the d_{302} spacing, obtained from the corresponding 2θ value, decreases from 3.941 Å (H-Beta, 2θ = 22.54°) to 3.897 Å (Si-Beta, 2θ = 22.80°) through dealumination, revealing the contraction of the BEA matrix. The d_{302} spacing of zeolite samples enlarges after the incorporation of Sn and the spacing increases with increasing the Sn loadings (i.e., from 3.897 Å for Si-Beta (2θ = 22.80°) to 3.927 Å for Sn-Beta-100 (2θ = 22.58°) and then to 3.945 Å for Sn-Beta-50 (2θ = 22.52°)). This is a clear evidence of BEA framework expansion, indicating the successful incorporation of Sn species into the framework of Beta zeolite.

The well-preserved miroporous BEA structure after dealumination and Sn incorporation can be further confirmed by the nitrogen physisorption (Figure S1), in which similar and typical type I adsorption/desorption isotherms can be observed for all the samples. On the other hand, the enhanced nitrogen uptake is clearly observed at high relative pressures $p/p_0 > 0.9$, which can be ascribed to the contributions of a large amount of interparticle voids originating from the disordered agglomeration of small crystallites of the zeolite Beta, and further confirmed by SEM (Figure S2). The postsynthesized Sn-Beta-50 samples appear as uniform nanoparticles with the average size of 80 nm, over 1 order of magnitude lower than the typical Sn-Beta samples prepared via hydrothermally route in the presence of HF.[27,29] Such small crystallites of the postsynthesized Sn-Beta zeolites are presumed to encounter less diffusion limitation in transferring bulky substrate molecules.

Table 1 summarizes the physicochemical properties of H-Beta, Si-Beta, and Sn-Beta samples. All the zeolite materials

Table 1. Physicochemical Properties of H-Beta, Si-Beta, and Metal-Containing Zeolites

catalyst	Si/Al[a]	Si/M[a]	surface area[b] ($m^2\ g^{-1}$)	micropore volume[c] ($cm^3\ g^{-1}$)
H-Beta	13.5		590	0.204
Si-Beta	>1800		620	0.210
Sn-Beta-100	>1800	97.0	600	0.202
Sn-Beta-50	>1800	51.3	580	0.200
Sn-Beta-40	>1800	41.8	570	0.198
Zr-Beta-50	>1800	51.9	573	0.197
Ti-Beta-50	>1800	52.1	575	0.198

[a]Determined by ICP. [b]Specific surface area obtained by BET method. [c]Calculated from *t*-plot.

have the similar BET surface area (570−590 $m^2\ g^{-1}$) and micropore volume (0.198−0.204 $cm^3\ g^{-1}$), suggesting the textural properties of Beta zeolite are well preserved after dealumination and Sn incorporation. Upon treatment with concentrated HNO_3, the n_{Si}/n_{Al} ratio of H-Beta sharply increases from 13.5 to over 1800 of dealuminated Si-Beta, suggesting the latter is essentially free of Al. After incorporation of Sn, the actual n_{Si}/n_{Sn} ratio determined by ICP is identical to the desired expected value, confirming the so-called dry impregnation method is an efficient strategy for the preparation of Sn(IV)-containing Beta zeolites.

On the basis of our previous work,[37] the dealumination of H-Beta and incorporation of Ti(IV) species were associated with the evolution of the silanols related to the vacant sites during postsynthesis. This phenomenon is also observed for preparing the Sn(IV)-containing zeolites using the dry impregnation method. The DRIFT spectrum (Figure 2) of parent H-Beta exhibits several characteristic bands in hydroxyl stretching region: one band at 3740 cm^{-1} ascribed to isolated external Si−OH groups, one band at 3600 cm^{-1} ascribed bridging hydroxyls Si−OH-Al, two bands at 3775 and 3655 cm^{-1} ascribed to Al−OH groups of extra-framework aluminum species, and one broad weak band centered at 3520 cm^{-1} ascribed to hydrogen-bonded Si−OH groups.[38,39] The dealumination procedure in

dx.doi.org/10.1021/cs500891s | ACS Catal. 2014, 4, 2801−2810

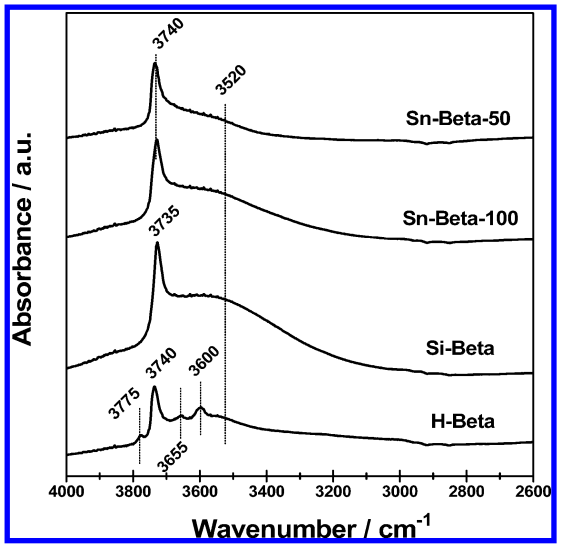


Figure 2. DRIFT spectra in the hydroxyl stretching vibration region of H-Beta, Si-Beta, Sn-beta-100, and Sn-Beta-50 samples.

concentrated HNO_3 solution is a well-established means to remove aluminum atoms from the framework of, in particular, Beta zeolite.[29−31,37] The treatment of H-Beta zeolite with concentrated HNO_3 solution results in the complete disappearance of three bands at 3775, 3655, and 3600 cm^{-1} associated with Al species (Figure 2), evidencing the complete elimination of Al from the framework, consistent with the ICP analysis results (n_{Si}/n_{Al} > 1800). Simultaneously, the intensification of the band at 3735 cm^{-1} due to isolated internal SiOH groups and the band at 3520 cm^{-1} related to hydrogen-bonded silanol groups are clearly observed, indicating the formation of vacant T atom sites (Scheme 1, dealumination step), in accordance with earlier assignments.[34,38,40] Dry impregnation of the obtained Si-Beta sample with Sn precursor (i.e., $(CH_3)_2SnCl_2$) leads to a decrease in the intensity of OH bands at 3735 and 3520 cm^{-1}, located in the vacant T atom sites, suggesting that Sn species react with these silanol groups and thus are incorporated into the Beta zeolite framework (Scheme 1, Sn incorporation step).

3.2. Existence States of Sn Species in Sn-Beta. Diffuse reflectance UV−vis analysis is first employed to understand the coordination states of Sn species incorporated. As shown in Figure 3, Sn-Beta-100 and Sn-Beta-50 samples both exhibit a

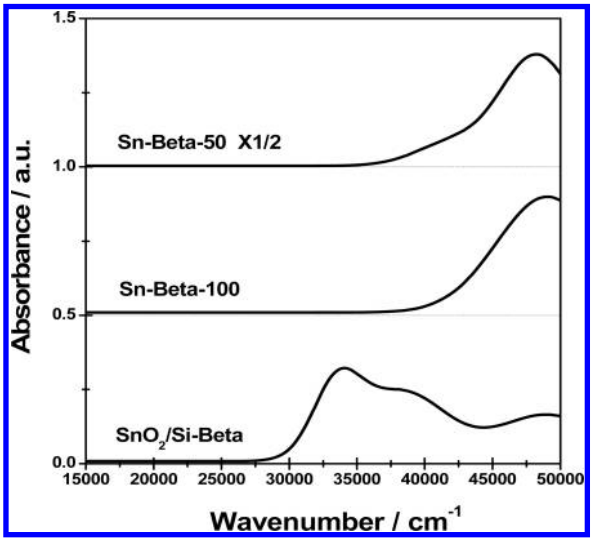
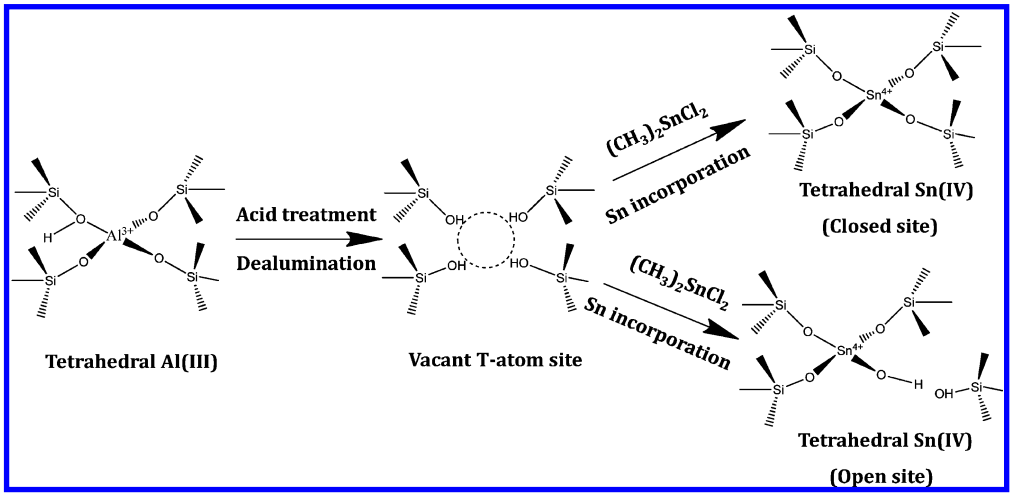


Figure 3. UV−vis spectra of dehydrated Sn-Beta and SnO_2/Si-Beta samples.

strong absorption band centered at ca. 48300 cm^{-1} (207 nm), arising from the ligand-to-metal charge transfer from O^{2-} to Sn^{4+}. This band has been generally assumed to be the catalytically active isolated Sn species in the framework with tetrahedral coordination,[27,29−31] and the intensity of this band increases distinctly with increasing Sn loading. For Sn-Beta-100, no distinct bands could be observed below 40 000 cm^{-1} (>250 nm), ruling out the existence of extra-framework bulk SnO_2 species.[29,30] For Sn-Beta-50, a very small shoulder could be observed at 35 000−40 000 cm^{-1}, probably due to the existence of small quantities of SnO_2 species. These results indicate that most Sn species could be incorporated into the framework of BEA via postsynthesis and exist in the highly isolated form, in great contrast to SnO_2/Si-Beta reference sample. The absence of crystalline SnO_2 aggregates in Sn-Beta samples is further evidenced by the invisible characteristic XRD diffraction peaks, for example, (110) at 2θ = 26.67° (Figure 1), and Raman vibrational modes, for example, A_{1g} at 632 cm^{-1} (Figure S3).

Scheme 1. Schematic Representation of the Incorporation of Tetrahedrally Coordinated Sn(IV) Species into Beta Zeolite



dx.doi.org/10.1021/cs500891s | ACS Catal. 2014, 4, 2801−2810

The existing states of Sn species in dehydrated Sn-Beta samples are investigated by XPS, and the results are shown in Figure 4. In the Sn 3d region, two signals positioned at 487.4

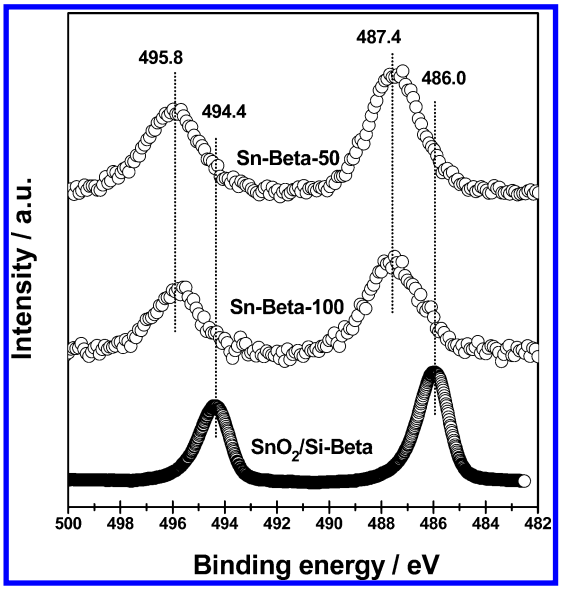


Figure 4. XPS of Sn-Beta and SnO_2/Si-Beta samples.

and 495.8 eV can be observed for both Sn-Beta-100 and Sn-Beta-50 samples, which should be ascribed to $3d_{5/2}$ and $3d_{3/2}$ photoelectrons of tetrahedrally coordinated framework Sn species.[41,42] In contrast, binding energy values of 486.0 and 494.4 eV, arising from $3d_{5/2}$ and $3d_{3/2}$ photoelectrons of octahedral Sn species, are clearly observed for SnO_2/Si-Beta, which is characteristic of Sn species existing in the form of SnO_2.[41,42] The XPS results reveal that Sn species in Sn-Beta samples are tetrahedrally coordinated in BEA framework via the dry impregnation method, in accordance with the results from UV−vis analysis.

^{119}Sn MAS NMR spectroscopy is further employed to provide a direct proof on the coordination states of Sn species in dehydrated Sn-Beta samples, and the results are shown in Figure 5. SnO_2/Si-Beta sample gives a main resonance signal at −604 ppm, corresponding to typical SnO_2 species in octahedral coordination. The NMR resonance signals of dehydrated Sn-Beta-100 and Sn-Beta-50 samples are observed at ca. −420 ppm, which should be originated from Sn species in a lower coordination state (i.e., tetrahedral Sn). The tetrahedral Sn species in the framework of BEA, Sn-Beta prepared via direct hydrothermal synthesis, was reported to give a resonance at −443 ppm by Corma et al.[18,43] Davis et al. further reported two resonance signals at −420 and −443 ppm in dehydrated Sn-Beta also prepared via direct hydrothermal synthesis: the former being ascribed to tetrahedral Sn in open arrangement and the latter to tetrahedral Sn in close arrangement.[44] Accordingly, the signal at −420 ppm observed for Sn-Beta in this study is ascribed to framework tetrahedral Sn in open arrangement, and the absence of signal at −604 ppm indicates that most Sn species have been successfully incorporated into BEA framework. It should be noted that hydration of tetrahedrally coordinated Sn species resulted in the formation of octahedral Sn species, as revealed by the NMR signal at ca. −685 ppm.[44] Considering that the open framework Sn species in Sn-Beta were proposed to be the active sites in Baeyer−Villiger oxidation of cyclic ketones,[45] the framework tetrahedral

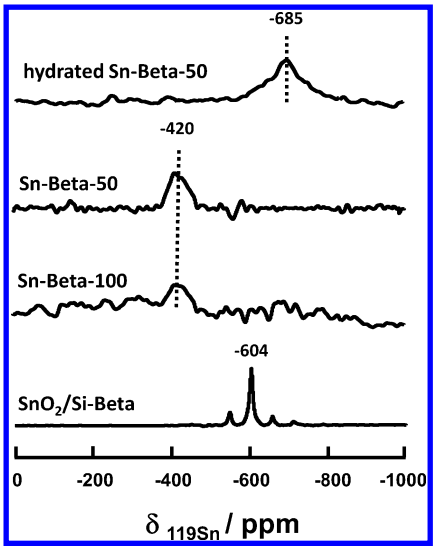


Figure 5. ^{119}Sn MAS NMR spectra of dehydrated and hydrated Sn-Beta and SnO_2/Si-Beta samples.

Sn species in open arrangement in our postsynthesized Sn-Beta might be active Lewis acid sites for various corresponding catalytic applications. On the basis of the characterization results, we further specify the scheme for the incorporation of tetrahedrally coordinated Sn(IV) species into Beta zeolite in open arrangement (Scheme 1).

Characterization results from UV−vis, XPS, and ^{119}Sn MAS NMR reveal that most Sn species have been successfully incorporated into the framework of Beta zeolite through the postsynthesis process and exist as isolated tetrahedral Sn in open arrangement (in dehydrated sample). Here, the use of organometallic dimethyltin dichloride as Sn precursor instead of tin(II)acetate, as employed by Hermans et al.,[31] could ensure a better incorporation of Sn into BEA structure, because the unsaturated Sn(II) species are very susceptible to oxygen during the preparation process and the formation of oxide-like species could be observed with a NMR signal at −604 ppm (Figure S4). The formation of oxidelike species in Sn-Beta would probably result in the low activity in various catalytic applications (vide infra, section 3.4). Compared with direct hydrothermal synthesis, the postsynthesis strategy appears to be simpler and easier to reproduce. More importantly, it is possible to obtain Sn-Beta nanocrystallines with high Sn loading via postsynthesis (Typical Sn loading in Sn-Beta prepared by direct hydrothermal synthesis is below 2.0 wt %.), which is crucial for catalytic applications.

3.3. Acidic Properties of Sn-Beta. FTIR analysis with pyridine adsorption allows a clear distinction between Brønsted and Lewis acid sites. As a good Lewis base, pyridine molecules can interact with the Brønsted acid sites forming pyridinium-ions, which are characterized by bands in the FTIR spectrum from 1512 to 1567 cm^{-1}. Pyridine molecules can also adsorb on the surface of Lewis acid sites through their isolated electron pair on nitrogen atoms, characterized by bands in the FTIR spectrum from 1423 to 1472 cm^{-1}.[39,46,47] Both Brønsted acid sites and Lewis acid sites can be observed for H-Beta samples, as shown in Figure S5. Although all the acid sites could be removed after complete dealumination (Si-Beta). The subsequent incorporation of metal ions (i.e., Sn^{4+}, Zr^{4+}, and Ti^{4+}) into Beta framework could create some Lewis acid sites, as confirmed by the FTIR bands at ∼1445 and 1605 cm^{-1} due to

dx.doi.org/10.1021/cs500891s | ACS Catal. 2014, 4, 2801−2810

pyridine adsorption (Figure 6). The pyridine adsorbed on Lewis sites could survive high-temperature evacuation (i.e., 573 K for Ti-Beta and 623 K for Sn-Beta and Zr-Beta), indicating the high strength of Lewis acid sites created. A quantitative analysis on the Lewis acid site densities of Sn-Beta, Ti-Beta, Zr-Beta probed by FTIR spectroscopy of pyridine adsorption and evacuation is shown in Figure 7. The Lewis acidity (i.e., the density and strength) created by metal ions incorporation could be determined as Sn-Beta > Zr-Beta > Ti-Beta, consistent with the results reported by Corma et al. from FTIR spectra of cyclohexanone adsorption.[19,48]

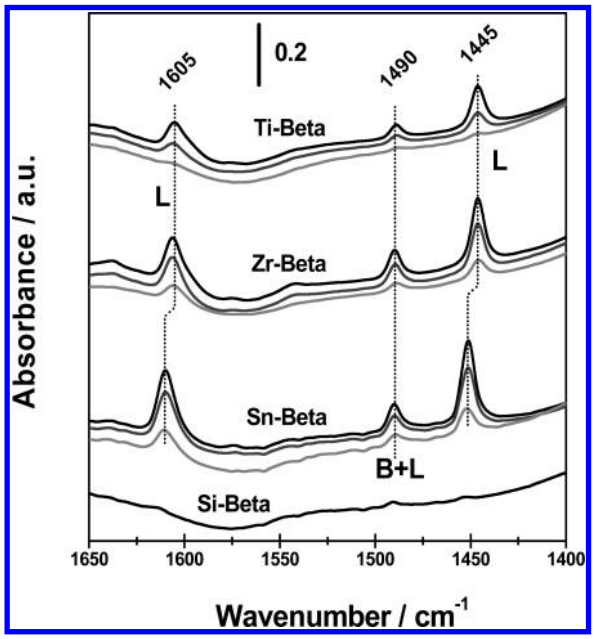


Figure 6. FTIR spectra of Si-Beta, Sn-Beta, Ti-Beta, and Zr-Beta samples after pyridine adsorption and evacuation at 473 (black line), 573 (dark gray line), and 623 K (gray line). B: Brønsted acid sites; L: Lewis acid sites.

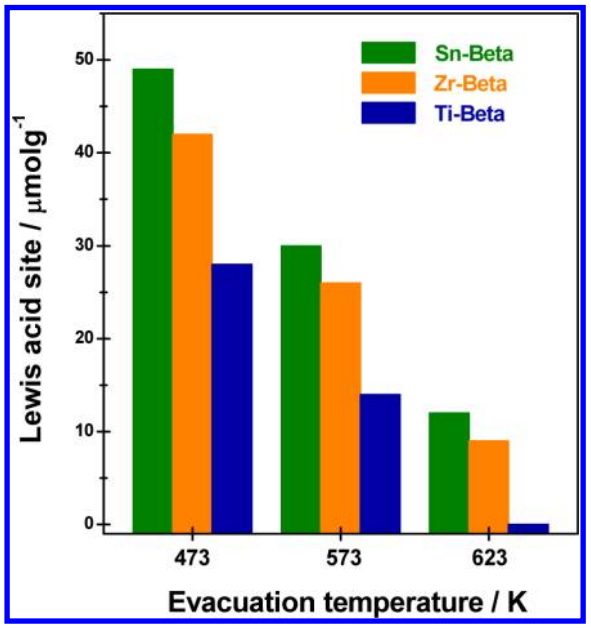


Figure 7. Lewis acid site densities of Sn-Beta, Ti-Beta, Zr-Beta probed by FTIR spectroscopy of pyridine adsorption and evacuation at different temperatures.

3.4. Catalytic Properties of Sn-Beta in Various Reactions. The catalytic performance of as-obtained Sn-Beta, together with some other Sn-Beta samples, is initially investigated in two typical model reactions, that is, Baeyer–Villiger oxidation of cyclohexanone with H_2O_2 and conversion of triose sugar dihydroxyacetone (DHA) into methyl lactate (LA), and the results are shown in Tables S1 and S2.

For the Baeyer–Villiger oxidation of cyclohexanone, our Sn-Beta-50 exhibited a similar productivity (1.08 $g_{lactone}\ g^{-1}{}_{cat}h^{-1}$) like 10 wt % Sn-Beta prepared by SSIE (1.07 $g_{lactone}g^{-1}{}_{cat}h^{-1}$), much higher than the hydrothermally synthesized one (0.37 $g_{lactone}g^{-1}{}_{cat}h^{-1}$, Table S1). As far as the productivity based on Sn is concerned, Sn-Beta-50 should be the most active one (31.7 $g_{lactone}\ g^{-1}{}_{Sn}h^{-1}$), followed by the hydrothermally synthesized one (24.6 $g_{lactone}\ g^{-1}{}_{Sn}h^{-1}$) and then the 10 wt % Sn-Beta prepared by SSIE (10.7 $g_{lactone}\ g^{-1}{}_{Sn}h^{-1}$). These results confirm the remarkable activity of our Sn-Beta sample in the Baeyer–Villiger oxidation reaction. The lower lactone selectivity can be ascribed to the existence of remaining silanol nests in the Sn-Beta-50 zeolite and such residual weak acid sites are capable to catalyze the hydrolysis of formed lactone to 6-hydroxycaproic acid.[31] For the conversion of DHA to LA, dry impregnated Sn-Beta-50 also exhibited very good activity as well as perfect product selectivity, and the productivity based on catalyst weight was comparable with the best results ever reported (Table S2). As far as productivity based on Sn is concerned, Sn-Beta with remarkable productivity of 23.8 $g_{LA}\ g^{-1}{}_{Sn}h^{-1}$ was several times more active than other Sn-zeolites prepared by different strategies.

In light of the above-mentioned results, it is clear that postsynthesized nanocrystalline Sn-Beta is a good solid Lewis acid catalyst for typical model reactions. The catalytic activities of postsynthesized nanocrystalline Sn-Beta zeolites, together with Zr-Beta and Ti-Beta zeolites, are further investigated in the ring-opening of cyclohexene oxide with stoichiometric mole of H_2O. In addition, the corresponding Si-Beta supported oxides (i.e., SnO_2/Si-Beta, ZrO_2/Si-Beta, and TiO_2/Si-Beta) are also prepared and evaluated for comparison. Under our reaction conditions, no product is obtained in the absence of catalyst, and very little product (<1%) is obtained using Si-Beta as catalyst, as shown in Table 2. Si-Beta supported metal oxides like SnO_2/Beta, ZrO_2/Beta, and TiO_2/Beta also exhibit very low activities in epoxide hydration. When Beta zeolites with framework incorporated metal ions (i.e., Sn^{4+}, Zr^{4+}, or Ti^{4+}) are employed as catalysts, considerable cyclohexene oxide conversion as well as high 1,2-diol selectivity can be obtained (ether from the dimerization as major byproduct). It is clear that the incorporation of metal ions in BEA framework is crucial to obtain the high catalytic activity in epoxide hydration. Under identical reaction conditions, Sn-Beta zeolites exhibit distinct higher catalytic activity than Zr-Beta and Ti-Beta with the same molar amount of metal ions. The activity difference should be correlated with the Lewis acid strength of the metal-containing zeolites in the sequence of Sn-Beta > Zr-Beta > Ti-Beta. The stronger Lewis acid is employed, the substrate molecule (i.e., cyclohexene oxide) is more efficiently activated on the Lewis acid sites, therefore leading to high catalytic activity. Moreover, Sn-Beta is obviously more active than the conventional Brønsted acid (Amberlite IR120) and Lewis base (Mg/Al-LDH) catalyst. Homogeneous Lewis acid catalyst $SnCl_4{\cdot}5H_2O$ is more active in the hydration of cyclohexene

dx.doi.org/10.1021/cs500891s | ACS Catal. 2014, 4, 2801–2810

Table 2. Hydration of Cyclohexene Oxide over Various Catalysts[a]

catalyst	Si/M[b]	conversion (%)[c]	selectivity (%)	reaction rate[d] (mmol h^{-1} g_{cat}^{-1})
Sn-Beta-50	51.3	90.2	92.7	15.0
Zr-Beta-50	51.9	34.5	91.0	5.8
Ti-Beta-50	52.1	13.7	95.0	2.3
SnO_2/Si-Beta	50.1	2.5	56.6	0.4
ZrO_2/Si-Beta	49.8	2.4	60.2	0.4
TiO_2/Si-Beta	50.1	2.8	53.8	0.5
$SnCl_4{\cdot}5H_2O$	/	73.5	80.5	12.3
H-Beta	13.5	45.9	89.5	6.4
Amberlite IR120		21.0	94.0	3.5
Mg/Al-LDH		<1.0		
Si-Beta	>1800	<1.0		
no catalyst		0		

[a]Reaction conditions: 10 mmol cyclohexene oxide, 20 mmol H_2O, 0.1 g catalyst, temperature = 313 K, reaction time = 6 h. [b]Determined by ICP. [c]Experimental accuracy of ±2% from GC analysis. [d]Average reaction rate within reaction time of 6 h.

oxide and high reaction rate of 12.3 mmol h^{-1} g_{cat}^{-1}, and a high 1,2-diol selectivity of 80.5% can be obtained; however, the Sn specific activity of $SnCl_4{\cdot}5H_2O$ is calculated to be 4294.6 mmol h^{-1} mol_{Sn}^{-1}, much lower than postsynthesized Sn-Beta-50 (46 272.6 mmol h^{-1} mol_{Sn}^{-1}). In addition, $SnCl_4{\cdot}5H_2O$ will hydrolyze during reaction in aqueous media and cannot be recycled, which is a common fatal shortcoming of such kind of Lewis acid catalysts.

The influence of preparation parameters (e.g., n_{Si}/n_{Sn} ratio and preparation methods) on the activity of Sn-Beta in cyclohexene oxide hydration reaction is investigated. As shown in Table 3, the n_{Si}/n_{Sn} ratio shows great impact on the catalytic performance of Sn-Beta in the ring-opening hydration of cyclohexene oxide. With increasing Sn loading in Sn-Beta (n_{Si}/n_{Sn} from 100 to 50), the conversion of cyclohexene oxide dramatically increases from 36.0 to 90.2%. However, only a margin increase in the cyclohexene oxide conversion (from 90.2 to 91.5%) can be achieved with further increasing Sn loading (n_{Si}/n_{Sn} from 50 to 40). The turnover frequency (TOF) is further calculated to reveal the intrinsic activity of catalyst samples. It is seen that similar TOF could be observed for Sn-Beta-50 (110.0 h^{-1}) and Sn-Beta-100 (105.9 h^{-1}), distinctly higher than that of Sn-Beta-40 (88.4 h^{-1}). This indicates the approaching saturation of framework Sn in Beta zeolite at n_{Si}/n_{Sn} of 50 and more Sn species will be forced to locate at the nonframework positions and form oxides, which show very low catalytic activity. Besides the n_{Si}/n_{Sn} ratio, both the preparation route and Sn precursor show great impact on the catalytic performance of Sn-Beta. It is seen that the outstanding catalytic performance of Sn-Beta can only be obtained through the precise combination of preparation route (DI, WI, or SSIE) and Sn precursor ($SnCl_4$ or $(CH_3)_2SnCl_2$) employed, demonstrating the superiority of the two-step postsynthesis strategy developed for the preparation of Sn-Beta in the present study.

Table 4 shows the effects of solvent employed on the catalytic performance of Sn-Beta-50 catalyst in the ring-opening hydration of cyclohexene oxide. Generally, the role of the solvents is to homogenize the liquid phase, thus reducing the mass-transfer problems to accelerate the interaction of reactants with catalyst. However, catalytic activity of Sn-Beta-50 catalyst is significantly suppressed when polar aprotic solvents (i.e., acetone, 1,4-dioxane, tetrahydrofuran, and acetonitrile) are employed in the reaction process. This should be due to the competing adsorption of solvent molecules on the catalytic active sites (i.e., Lewis acid sites), which might hinder the interaction between the catalytic active sites and the reactants molecules. In this context, the higher basicity of solvent employed, the higher hinder effects could be observed. To confirm this speculation, different solvents were added into the reaction system after reaction of 1 h, and their negative impacts could be clearly observed (Figure S6).

Table 4. Influence of Solvent on the Cyclohexene Oxide Hydration over Sn-Beta-50[a]

solvent	conversion (%)[b]	selectivity (%)	reaction rate[c] (mmol h^{-1} g_{cat}^{-1})
none	90.2	92.7	15.0
acetone	78.0	92.1	13.0
1,4-dioxane	63.8	90.6	10.6
tetrahydrofuran	45.5	92.9	7.6
acetonitrile	12.6	89.5	2.1

[a]Reaction conditions: 10 mmol cyclohexene oxide, 20 mmol H_2O, 20 mmol solvent, 0.1 g of catalyst, temperature = 313 K, reaction time = 6 h. [b]Experimental accuracy of ±2% from GC analysis. [c]Average reaction rate within reaction time of 6 h

To assess the true heterogeneity of the Sn-Beta catalyst, hot-filtration based leaching test is performed to determine if Sn^{4+} ions can leach from the catalyst into the reaction mixture and

Table 3. Influence of n_{Si}/n_{Sn} Ratio and Preparation Method on the Hydration of Cyclohexene Oxide[a]

catalyst	preparation method[b]	Si/Sn[c]	Lewis acid site (μmol g^{-1})[d]	conversion (%)[e]	selectivity (%)	reaction rate[f] (mmol h^{-1} g_{cat}^{-1})	TOF (h^{-1})[g]
Sn-Beta-40	DI; Me_2SnCl_2	41.8	51	91.5 (33.5)	92.5	15.3	88.4
Sn-Beta-50	DI; Me_2SnCl_2	51.3	49	90.2 (30.6)	92.7	15.0	110.0
Sn-Beta-100	DI; Me_2SnCl_2	97.0	34	36.0 (16.8)	92.3	6.0	105.9
Sn-Beta-50	DI; $SnCl_4$	49.8	46	22.8 (11.3)	80.8	3.8	40.6
Sn-Beta-50	WI; Me_2SnCl_2	51.2	38	13.1 (7.2)	84.4	2.2	25.9
Sn-Beta-50	WI; $SnCl_4$	49.3	19	16.4 (8.9)	84.1	2.7	31.9
Sn-Beta-50	SSIE; $Sn(OAc)_2$	49.5	53	44.2 (17.3)	90.6	7.4	62.2
Sn-Beta-150[h]	HT; $SnCl_4$	148.7	21	32.5 (14.2)	91.8	5.4	126.7

[a]Reaction conditions: 10 mmol cyclohexene oxide, 20 mmol H_2O, 0.1 g of catalyst, temperature = 313 K, reaction time = 6 h. [b]DI: dry impregnation, WI: wet impregnation, SSIE: solid-state ion-exchange, HT: hydrothermal. [c]Determined by ICP. [d]Determined by FTIR spectroscopy of pyridine adsorption followed by evacuation at 473 K. [e]Values in parentheses indicate the conversion after reaction of 1 h, based on which the TOF is calculated. Experimental accuracy of ±2% from GC analysis. [f]Average reaction rate within reaction time of 6 h. [g]Calculated as mole of cyclohexene oxide converted per hour per mole of Sn. [h]Synthesized according to Corma's method and kindly provided by Prof. Peng Wu.[29]

dx.doi.org/10.1021/cs500891s | ACS Catal. 2014, 4, 2801−2810

possibly participate in the catalytic reaction. The catalyst is removed from the reaction mixture by centrifugation after the reaction time of 1 h, and the filtrate proceeds by itself for another 5 h under identical conditions. As shown in Figure 8,

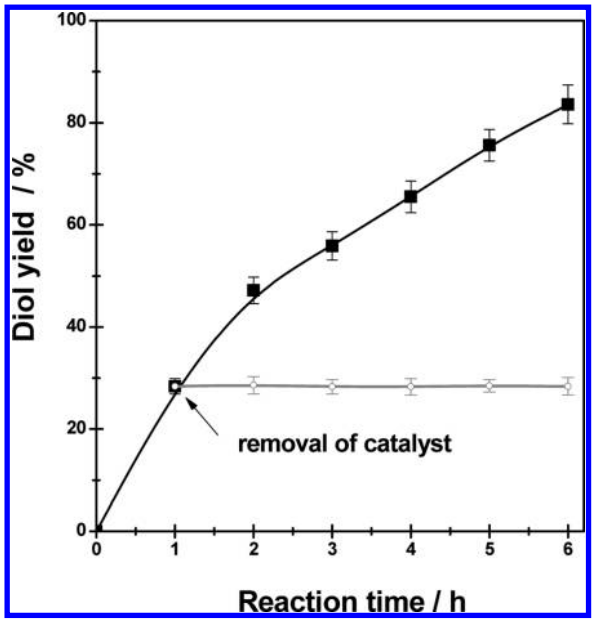


Figure 8. 1,2-Diol yield in the ring-opening of cyclohexene oxide on Sn-Beta-50, plotted as a function of reaction time. Reaction conditions: 10 mmol cyclohexene oxide, 20 mmol H_2O, 0.1 g of catalyst, temperature = 313 K.

the removal of the catalyst leads to complete termination of the reaction, confirming the heterogeneous nature of the Sn-Beta catalyst in the ring-opening hydration of cyclohexene oxide.

The recycling ability of Sn-Beta-50 catalyst is investigated, and the results are shown in Figure 9. A gradual decrease in the activity (e.g., cyclohexene oxide conversion from 90.2 to 59.5%) could be observed within four cycles if Sn-Beta catalyst was just centrifuged for reuse. However, if the catalyst sample was washed with acetone and further calcined for reuse, its catalytic activity could be fully recovered, and no significant changes in the catalytic activity or idol selectivity could be observed in the

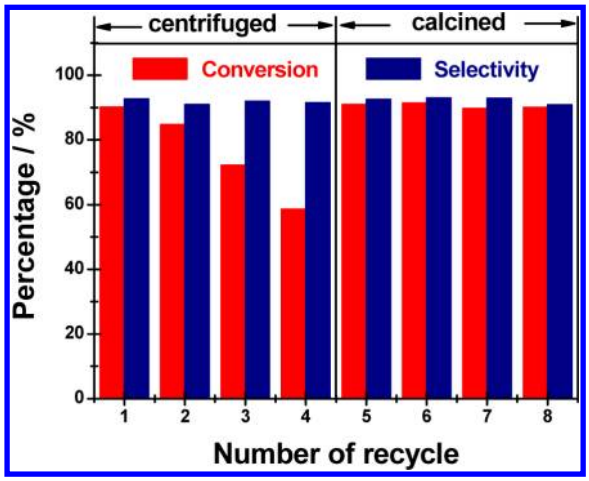


Figure 9. Recycling test for cyclohexene oxide hydration catalyzed by Sn-Beta-50. Reaction conditions: 10 mmol cyclohexene oxide, 20 mmol H_2O, 0.1 g of catalyst, temperature = 313 K, reaction time = 6 h.

next four cycles. The possible leaching of Sn species during reaction can be excluded from element analysis, and the possible changes in the textural properties of Sn-Beta after recycles could be ruled out according to the XRD and surface area analysis. In this context, the decrease in the catalytic activity should be due to the block of active sites by bulky byproducts, and the removal of these species can completely regenerate the catalyst. On the whole, postsynthesized Sn-Beta is a potential heterogeneous catalyst for future application in the ring-opening of epoxides if a suitable regeneration process is employed.

3.5. Ring-Opening Hydration of Epoxides Catalyzed by Lewis Acid. The ring-opening hydration of epoxides catalyzed by Brønsted acid has been well studied in the past. In the present study, it is verified that the ring-opening hydration of epoxide can also be catalyzed by water-tolerant Lewis acid. A direct comparison between H-Beta and Sn-Beta is made to disclose the superiority of solid Lewis acid to conventional Brønsted acid in this reaction. The apparent activation energies, calculated using the Arrhenius equation, are 34.8 and 55.5 kJ mol^{-1} catalyzed by Sn-Beta and H-Beta, respectively (Figure 10). The much lower apparent activation energy obtained on

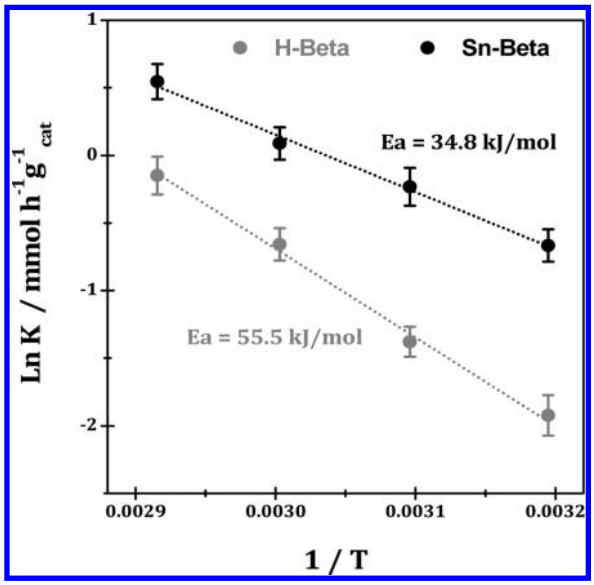


Figure 10. Plots of apparent activation energy in the hydration of cyclohexene oxide catalyzed by H-Beta and Sn-Beta.

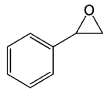
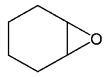
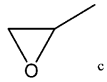
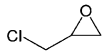
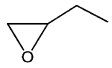
Sn-Beta than that on H-Beta reveals that solid Lewis acid site created by Sn incorporation into BEA structure is better candidate for the ring-opening hydration of epoxide.

On the basis of the above-mentioned results, we further applied Sn-Beta in the ring-opening hydration of different epoxide substrates (Table 5). It is seen that high activity can be obtained for the hydration of all epoxide substrates, whereas the selectivity to 1,2-diols is somewhat different. Generally, epoxide molecules with small dynamic sizes can accumulate in the channel of BEA zeolite and react with each other to produce undesired byproducts, resulting in the decrease in selectivity toward 1,2-diols to some extent. In contrast, epoxide substrates with large dynamic size are subject to severe stereoconfinement, which effectively suppresses the formation of byproducts, and, therefore, improves the yield of 1,2-diols.

It is also found that the epichlorohydrin undergoes catalytic reaction more slowly than styrene oxide under the same

dx.doi.org/10.1021/cs500891s | ACS Catal. 2014, 4, 2801−2810

Table 5. Hydration of Different Epoxide Substrates Catalyzed by Sn-Beta-50 Catalyst[a]

Substrate	Temperature (K)	Time (h)	Epoxide conversion (%) [b]	1,2-Diol selectivity (%)
	313	1.5	> 99.5	> 99.9
	313	6	90.2	92.7
 [c]	313	6	75.3	74.7
 [c]	313	8	50.1	71.9
	313	6	43.0	90.8
	313	8	45.5	93.5

[a]Reaction conditions: 10 mmol epoxide, 20 mmol H_2O, 0.1 g of catalyst. [b]Experimental accuracy of ±2% from GC analysis. [c]Reaction was performed in a 10 mL autoclave under N_2 pressure (1.0 MPa).

reaction conditions. Similar results have been observed for the epoxide ring-opening reaction using mesoporous SBA-15 supported Fe(III) catalysts.[49] The difference in reactivity can be attributed to the steric and electronic difference among the substrate molecular, which accordingly affects the ring-opening mechanism (see discussion in the Supporting Information).

4. CONCLUSION

In this study, a simple and scalable two-step synthesis procedure has been developed to prepare Sn-Beta zeolites. Briefly, in the first step, commercial H-Beta zeolites are treated in concentrated nitric acid solution to result in Si-Beta, and vacant T sites with associated silanol groups are created. In the second step, the organometallic Sn precursor $(CH_3)_2SnCl_2$ interacts with vacant T sites in the Si-Beta zeolite, and Sn species are subsequently incorporated into the framework of Beta zeolite upon calcination. The preparation procedure is monitored by means of XRD and DRIFT analysis. Exclusive tetrahedral coordinated Sn species in the BEA framework in open arrangement are clearly evidenced by characterization results from UV−vis, XPS, and ^{119}Sn MAS NMR analysis. The postsynthesis procedure developed here is considered as an attractive strategy to fabricate Sn-Beta nanocrystallines with high Sn loading.

The acidity of parent H-Beta and metal ions incorporated Si-Beta is investigated by FTIR spectroscopy with pyridine adsorption. Lewis acid sites are created on the basis of the metal ion incorporation, and the Lewis acidity is observed to be Sn-Beta > Zr-Beta > Ti-Beta. The obtained Sn-Beta zeolites are studied as potential catalysts in the ring-opening hydration of epoxides to the corresponding 1,2-diols. Remarkably high catalytic activity as well as high 1,2-diol selectivity could be achieved in the ring-opening hydration of cyclohexene oxide with a H_2O/epoxide molar ratio of 2:1 at near ambient and solvent-free conditions. Lewis acid Sn-Beta exhibits a distinct higher catalytic activity than H-Beta in the ring-opening hydration of cyclohexene oxide with a much lower apparent activation energy of 34.8 kJ mol^{-1} compared with 55.5 kJ mol^{-1} of H-Beta, whereas the catalytic activities of different metal ion incorporated Si-Beta samples (i.e., Sn-Beta, Zr-Beta, and Ti-Beta, are determined by their Lewis acidity. The hot-filtration and recycling experiments reveal the true heterogeneity and perfect stability of Sn-Beta zeolites during reaction. Sn-Beta zeolites also exhibit good catalytic performance in the ring-opening hydration of different epoxide substrates. All these issues demonstrate the great potential of Sn-Beta Lewis acids for various catalytic applications. Moreover, the preparation parameters of Sn-Beta zeolites are most important, and the combination of dry impregnation route and organometallic $(CH_3)_2SnCl_2$ as Sn precursor appears to be the unique and feasible strategy to obtain the robust Sn-Beta catalysts.

■ ASSOCIATED CONTENT

Supporting Information

Additional characterization and catalytic results. This material is available free of charge via the Internet at http://pubs.acs.org/

■ AUTHOR INFORMATION

Corresponding Author

*E-mail : lild@nankai.edu.cn. Fax/Tel.:+ 86-22-23500341.

Notes

The authors declare no competing financial interest.

dx.doi.org/10.1021/cs500891s | ACS Catal. 2014, 4, 2801−2810

■ ACKNOWLEDGMENTS

This work is financially supported by the National Natural Science Foundation of China (21373119) and the Ministry of Education of China (NCET-11-0251, IRT13022, IRT13R30). The support from 111 Project (B12015) and the Collaborative Innovation Center of Chemical Science and Engineering (Tianjin) are also acknowledged. Furthermore, M.H. wants to acknowledge financial support by Deutsche Forschungsgemeinschaft.

■ REFERENCES

(1) Huang, J. H.; Akita, T.; Faye, J.; Fujitani, T.; Takei, T.; Haruta, M. *Angew. Chem., Int. Ed.* **2009**, *48*, 7862−7866.
(2) Saikia, L.; Satyarthi, J. K.; Srinivas, D.; Ratnasamy, P. *J. Catal.* **2007**, *252*, 148−160.
(3) Kore, R.; Srivastava, R.; Satpati, B. *ACS Catal.* **2013**, *3*, 2891−2904.
(4) Seidel, A. *Kirk-Othmer Encyclopedia of Chemical Technology*; Wiley: New York, 2005.
(5) Reed, L. M.; Wenzel, L. A.; O'Hara, J. B. *Ind. Eng. Chem.* **1956**, *48*, 205−208.
(6) Shvets, V. F.; Kozlovskiy, R. A.; Kozlovskiy, I. A.; Makarov, M. G.; Suchkov, J. P.; Koustov, A. V. *Org. Process Res. Dev.* **2005**, *9*, 768−773.
(7) Strickler, G. R.; Landon, V. G.; Lee, G. J. U.S. Patent 6,211,419, April 3, 2001.
(8) Van Kruchten, E. M. G. A.; Derks, W. U.S. Patent 6,580,008, June 17, 2003.
(9) Kawabe, K. U.S. Patent 6,080,897, June 27, 2000.
(10) Van Kruchten, E. M. G. A.; U.S. Patent 5874653, February 23, 1999.
(11) Van Kruchten, E. M. G. A.; W.O. Patent 9923053, May 14, 1999.
(12) Van Hal, J. W.; Ledford, J. S.; Zhang, X. *Catal. Today* **2007**, *123*, 310−315.
(13) Li, Y. C.; Yan, S. R.; Yue, B.; Yang, W. M.; Xie, Z. K.; Chen, Q. L.; He, H. Y. *Appl. Catal., A* **2004**, *272*, 305−310.
(14) Li, Y. C.; Yan, S. R.; Qian, L. P.; Yang, W. M.; Xie, Z. K.; Chen, Q. L.; Yue, B.; He, H. Y. *J. Catal.* **2006**, *241*, 173−179.
(15) Li, B.; Bai, S. Y.; Wang, X. F.; Zhong, M. M.; Yang, Q. H.; Li, C. *Angew. Chem., Int. Ed.* **2012**, *51*, 11517−11521.
(16) Corma, A.; Garcia, H. *Chem. Rev.* **2003**, *103*, 4307−4366.
(17) Román-Leshkov, Y.; Davis, M. E. *ACS Catal.* **2011**, *1*, 1566−1580.
(18) Corma, A.; Nemeth, L. T.; Renz, M.; Valencia, S. *Nature* **2001**, *412*, 423−425.
(19) Corma, A.; Domine, M. E.; Nemeth, L.; Valencia, S. *J. Am. Chem. Soc.* **2002**, *124*, 3194−3195.
(20) Moliner, M.; Román-Leshkov, Y.; Davis, M. E. *Proc. Nat. Acad. Sci. U.S.A.* **2010**, *107*, 6164−6168.
(21) Román-Leshkov, Y.; Moliner, M.; Labinger, J. A.; Davis, M. E. *Angew. Chem., Int. Ed.* **2010**, *49*, 8954−8957.
(22) Holm, M. S.; Saravanamurugan, S.; Taarning, E. *Science* **2010**, *328*, 602−605.
(23) Gunther, W. R.; Wang, Y.; Ji, Y.; Michaelis, V. K.; Hunt, S. T.; Griffin, R. G.; Román-Leshkov, Y. *Nat. Commun.* **2012**, *3*, 1109.
(24) Dusselier, M.; Van Wouwe, P.; Dewaele, A.; Makshina, E.; Sels, B. F. *Energy Environ. Sci.* **2013**, *6*, 1415−1442.
(25) Taarning, E.; Saravanamurugan, S.; Holm, M. S.; Xiong, J.; West, R. M.; Christensen, C. H. *ChemSusChem* **2009**, *2*, 625−627.
(26) Valencia, S.; Corma, A. U.S. Patent 5,968,473A, October 19, 1999.
(27) Paris, C.; Moliner, M.; Corma, A. *Green Chem.* **2013**, *15*, 2101−2109.
(28) Chang, C.-C.; Wang, Z.; Dornath, P.; Je Cho, H.; Fan, W. *RSC Adv.* **2012**, *2*, 10475−10477.
(29) Li, P.; Liu, G. Q.; Wu, H. H.; Liu, Y. M.; Jiang, J. G.; Wu, P. *J. Phys. Chem. C* **2011**, *115*, 3663−3670.
(30) Dijkmans, J.; Gabriëls, D.; Dusselier, M.; Clippel, F.; Vanelderen, P.; Houthoofd, K.; Malfliet, A.; Pontikes, Y.; Sels, B. F. *Green Chem.* **2013**, *15*, 2777−2785.
(31) Hammond, C.; Conrad, S.; Hermans, I. *Angew. Chem., Int. Ed.* **2012**, *51*, 11736−11739.
(32) Wolf, P.; Hammond, C.; Conrad, S.; Hermans, I. *Dalton Trans.* **2014**, *43*, 4514−4519.
(33) Emeis, C. A. *J. Catal.* **1993**, *141*, 347−354.
(34) Dzwigaj, S.; Janas, J.; Gurgul, J.; Socha, R. P.; Shishido, T.; Che, M. *Appl. Catal., B* **2009**, *85*, 131−138.
(35) Srebowata, A.; Baran, R.; Lomot, D.; Lisovytskiy, D.; Onfroy, T.; Dzwigaj, S. *Appl. Catal., B* **2014**, *147*, 208−220.
(36) Treacy, M. M. J.; Newsam, J. M. *Nature* **1988**, *332*, 249−251.
(37) Tang, B.; Dai, W.; Sun, X.; Guan, N.; Li, L.; Hunger, M. *Green Chem.* **2014**, *16*, 2281−2291.
(38) Nogier, J. P.; Millot, Y.; Man, P. P.; Shishido, T.; Che, M.; Dzwigaj, S. *J. Phys. Chem. C* **2009**, *113*, 4885−4889.
(39) Li, L.; Guan, N. *Microporous Mesoporous Mater.* **2009**, *117*, 450−457.
(40) Dzwigaj, S.; Millot, Y.; Krafft, J. M.; Popovych, N.; Kyriienko, P. *J. Phys. Chem. C* **2013**, *117*, 12552−12559.
(41) Pachamuthu, M. P.; Shanthi, K.; Luque, R.; Ramanathan, A. *Green Chem.* **2013**, *15*, 2158−2166.
(42) Luo, H. Y.; Bui, L.; Gunther, W. R.; Min, E.; Román-Leshkov, Y. *ACS Catal.* **2012**, *2*, 2695−2699.
(43) Renz, M.; Blasco, T.; Corma, A.; Fornés, V.; Jensen, R.; Nemeth, L. *Chem.—Eur. J.* **2002**, *8*, 4708−4717.
(44) Bermejo-Deval, R.; Assary, R. S.; Nikolla, E.; Moliner, M.; Román-Leshkov, Y.; Hwang, S. J.; Palsdottir, A.; Silverman, D.; Lobo, R. F.; Curtiss, L. A.; Davis, M. E. *Proc. Nat. Acad. Sci. U.S.A.* **2012**, *109*, 9727−9732.
(45) Boronat, M.; Concepción, P.; Corma, A.; Renz, M.; Valencia, S. *J. Catal.* **2005**, *234*, 111−118.
(46) Buzzoni, R.; Bordiga, S.; Ricchiardi, G.; Lamberti, C.; Zecchina, A.; Bellussi, G. *Langmuir* **1996**, *12*, 930−940.
(47) Guo, Q.; Fan, F.; Pidko, E. A.; van der Graaff, W. N. P.; Feng, Z.; Li, C.; Hensen, E. J. M. *ChemSusChem* **2013**, *6*, 1352−1356.
(48) Corma, A.; Domaine, M. E.; Valencia, S. *J. Catal.* **2003**, *215*, 294−304.
(49) Das, S.; Asefa, T. *ACS Catal.* **2011**, *1*, 502−510.